MELBA Journal Machine Learning for Biomedical Imaging

A multi-site loiasis dataset of whole blood videos

Linda Djune-Yemeli [1,*], Rella Zoleko-Manego [2], Charles B. Delahunt [3,4,*], Donald F. Fankam [1], Yannick Y. Nzeuhang [1], Jean G. Bopda [1], Mbakam S. Laetitia [1], Yves A. Balog [1], Steve M. Tchana [1], Ghyslain Mombo-Ngoma [2,6], Michael Ramharter [2,6,7], Maria Diaz de Leon Derby [5], Zaina L. Moussa [5], Ethan Spencer [4], Dipayan Banik [4], Matthew D. Keller [4], Karla N. Fisher [8,9], Daniel A. Fletcher [5], Isaac I. Bogoch [8,9,10], Anne-Laure Le Ny [4], Saskia Deda Davi [2,6,11,12], Joseph Kamgno [1]

1 Higher Institute for Scientific and Medical Research (ISM), Yoaoundé, Cameroon **2** Centre de Recherches Médicale de Lambaréné, Gabon (CERMEL) **3** University of Washington, Seattle, Washington **4** Formerly at Global Health Labs, Inc, Bellevue, Washington (ceased operations in 2025) **5** Department of Bioengineering, University of California, Berkeley, Berkeley, California **6** Center for Tropical Medicine, Bernhard Nocht Institute for Tropical Medicine & I. Dept. of Medicine University Medical Center Hamburg-Eppendorf (BNITM), Hamburg, Germany **7** German Center for Infection Research (DZIF), Partner Site Hamburg-Lübeck-Borstel-Riems, Hamburg, Germany **8** Division of General Internal Medicine, Toronto General Hospital, University Health Network, Toronto, Canada **9** Division of Infectious Diseases, Toronto General Hospital, University Health Network, Toronto, Canada **10** Department of Medicine, University of Toronto, Toronto, Canada **11** Department for Infectious Disease and Tropical Medicine, University Hospital Heidelberg, Heidelberg, Germany **12** German Center for Infection Research (DZIF), Partner Site Heidelberg, Heidelberg, Germany.
* denotes equal contribution
joseph.kamgno@ismcm.org, rella.zoleko@cermel.org, delahunt@uw.edu

Abstract

Loiasis is a blood-borne filarial infection under consideration for inclusion in the WHO's priority list of Neglected Tropical Diseases. In addition to its direct impact on human health, loiasis frequently occurs as a co-infection with other filarial diseases, including onchocerciasis (river blindness) and lymphatic filariasis (LF, elephantiasis). This overlapping geographic distribution seriously hinders mass drug administration (MDA) with ivermectin (IVM) for onchocerciasis and LF control, because individuals with *Loa loa* microfilarial (mf) loads exceeding 30,000 mf/mL are at high risk of developing severe adverse events, including coma and death, following IVM treatment. Therefore, safe MDA in loiasis co-endemic areas requires active detection and exclusion of high *L. loa* mf individuals from treatment, the so-called Test and Not Treat (TaNT) strategy. Automated, AI-driven diagnostics have shown strong potential to enhance TaNT implementation and fill a crucial care need for underserved populations, yet important performance limitations remain. To support AI research for the pressing health care needs of filarial diseases, we release this first-of-its-kind dataset to enable development of AI algorithms for detecting *L. loa* in whole blood samples. The dataset includes 33,000 videos of whole blood in capillaries, in 4705 sessions (7 videos per session) from 1948 patients, captured by NTDscope portable imaging devices during four studies in 2023 and 2025 in Cameroon and Gabon. The videos contain a range of *L. loa* microfilariae counts and negative cases, as well as some cases with *Mansonella perstans*, another tropical filarial parasite. The metadata include expert microfilariae counts from Giemsa-stained blood films for each patient.

Keywords

Loa loa, Mansonella, neglected tropical disease, mobile microscopy, machine learning

Article informations

https://doi.org/10.59275/j.melba.2026-b66d

Volume 2026, Received: 2026-06-19, Published 2026-09-21

Corresponding author: joseph.kamgno@ismcm.org, rella.zoleko@cermel.org, delahunt@uw.edu
Special issue: MICCAI Open Data 2026 x MELBA
Guest editors: AT, MS et al.

1. Background

Loiasis is an emerging Neglected Tropical Diseases (NTDs) endemic in West and Central African rainforest areas (Kelly-Hope et al., 2012; Metzger and Mordmüller, 2014; Ramharter et al., 2024). The disease is caused by the filarial nematode *Loa loa*, transmitted to humans through the bite of the tabanid fly Chrysops (Boussinesq, 2006). Epidemiological data estimated that over 14 million individuals are at risk of infection, with an estimated 10 million cases (Metzger and Mordmüller, 2014). Loiasis causes a wide range of clinical symptoms, from none at all to severe complications, including transient angioedema (Calabar swelling), ocular migration of the adult parasite under the conjunctiva (eye worm) (Boussinesq, 2006), and encephalitis, associated with high microfilariae (mf) densities (>30,000 mf/mL) (Gardon et al., 1997). Other symptoms involving deep organs (lung, heart, kidney) and excess mortality have been reported (Buell et al., 2016; Chesnais et al., 2017). Loiasis is under consideration for inclusion in the WHO's priority list of Neglected Tropical Diseases (Jacobsen et al., 2022; WHO, 2025a, 2001).

Loiasis is often co-endemic with onchocerciasis (river blindness). This overlapping geographic distribution seriously hinders mass drug administration (MDA) with ivermectin (IVM) for effective control of onchocerciasis. Notably, ivermectin treatment can cause catastrophic, even fatal, side effects in persons with high *L. loa* infections (>30,000 mf/uL). Therefore, safe MDA in co-endemic areas requires active detection and exclusion of high *L. loa* mf individuals from treatment, the so-called Test and Not Treat (TaNT) strategy (Gardon et al., 1997; Boussinesq et al., 2003; Boulle et al., 2025; Pion, 2020). TaNT depends on accurate, point-of-care diagnostics, the development of more efficient tools has become an urgent priority (diagnosis via Giemsa-stained blood films is neither rapid nor point-of-care).

2. Summary

Automated, AI-driven diagnostics have shown strong potential to greatly improve TaNT and fill a crucial care need for underserved populations. However, to our knowledge no datasets exist for rapid diagnosis of loaisis (or filariasis) in whole blood, and the only existing automated diagnostic operating on this type of whole blood sample has known performance gaps (Djune-Yemeli et al., 2026). Therefore, we release this AI-ready dataset to enable development of AI algorithms to better detect *L. loa* in whole blood samples.

The dataset contains over 33,000 mp4 videos of whole blood in capillaries from 4705 diagnostic sessions collected in four field studies in Cameroon and Gabon, as well as relevant metadata (e.g. filarial load ground truth). The videos were captured by the NTDscope (de Leon Derby et al., 2025), which is a next-generation version of the CellScope (D'Ambrosio et al., 2015).

We hope that AI researchers can use this dataset, plus the description of the clinical context, to develop clinically-deployable algorithms that pair with hardware such as the NTDscope to effectively address the long-neglected health care challenge of *L. loa* and other filarial infections.

3. Discussion

This dataset, the first of its kind, offers sufficient data (1,948 patients and over 33,000 videos) to train and validate current-generation AI algorithms. Its four studies and five sites are drawn from populations in endemic regions, spanning ages 5 to 89+, with balanced gender mix, and with a full range of filarial loads including 65 patients with high-risk loads. The data also includes *M. perstans* infections, enabling speciation algorithms.

Limitations: All videos are from one device type, and there are no lymphatic filariasis cases. There are no object-location annotations; the ground truth consists of (i) filarial counts from Giemsa-stained blood films and (ii) per-video manual counts.

4. Resource Availability

4.1 Clinical Use Cases

Effective algorithms could improve care in several important use cases, if the AI development is informed, from the beginning, by clinicians and the clinical use case – their needs and constraints. Some use cases and their target performance requirements are as follows:

1. TaNT (*L. loa*, Test and Not Treat): The crucial requirement of this use case is to distinguish between "Not Treat" high microfilaremia infection (i.e. >30,000 mf/mL) vs "Treat" low microfilaremia infection (including negative cases). The 2026 algorithm used a threshold of 20,000 mf/mL to provide a margin of safety detecting patients with Giemsa reads >30,000 mf/mL. A False Negatives (i.e. a high microfilaremia mistakenly labeled as low microfilaremia and therefore eligible for ivermectin) incur high cost: they create risk of a serious adverse event (SAE) with harm to the patient. False Positives (i.e. lower microfilaremia mistakenly labeled as "Not Treat") carry a (lower) cost in that patients who could receive ivermectin are instead routed into other care channels. Note that correct diagnosis of negatives (0 mf/mL) vs low- microfilaremia infection is irrelevant for this use case. However, certain subpopulations (e.g. males age 31-40) may warrant "Not Treat" status at lower microfilaremias (Boulle et al., 2025).

A result delivered within 2 or 3 minutes of video capture is needed to support clinical care workflow. Since compute hardware is constrained by device price-point and portability, this time-to-result may constrain model options and might also force image downsampling.

2. Mapping The goal of this use case is to support spatial mapping of *L. loa*, to inform MDA programs. This task requires quantitation at all levels of filaremia, since in endemic areas a majority of infected individuals carry fewer than 8,000 mf/mL e.g. (Veletzky et al., 2024). It also requires distinguishing zero mf counts (i.e. True Negatives in the usual parasitemia sense). Community Micro-Filarial Load (equivalently the Williams Geometric Mean) (Kamtchum and alia, 2014) uses the formula

$$CMFL = exp\left(\frac{\Sigma_i\ ln(x_i + 1)}{n}\right) - 1$$

where x_i = filaremia for case i, n = number of cases, and the sum is over all cases. The required accuracy depends on how sensitive the CMFL formula, in context, is to errors in the input counts x_i. An important caveat (not addressable with this dataset) for diagnostics that rely solely on microfilarial counts is that in endemic areas a large fraction of infected individuals exhibit no detectable microfilariae (Veletzky et al., 2024); these amicrofilaremic cases would be systematically missed. Separately, the RAPLOA method is mainly used to characterize areas as high or low risk for SAEs, and considers only the presence of adult worm in the eye (Chesnais et al., 2017; Ramharter et al., 2024).

3. Lymphatic Filariasis (LF) Lymphatic filariasis (Goldin and Juergens, 2025; WHO, 2025b) also presents mf in blood similarly to *L. loa* (but only during night-time). The NTDscope device is potentially useful for detection of LF (unpublished data). However, LF has generally much lower filaremia (often $<$ 200 mf/mL), and thus requires diagnostics with very low LoD. This implies a different algorithm optimization target than for TaNT or *L. loa* mapping. Time-to-result: within 2 – 3 minutes of video capture.

4. Speciation Distinguishing *L. loa* from *M. perstans* has value for two reasons: To distinguish low-microfilaremia mono-infections of Loa loa from M. perstans (for accurate *L. loa* mapping purposes); and also to better study the two illnesses for their own sakes. To a first approximation, distinguishing the two species is not relevant to TaNT, because *M. perstans* filaria is in general low, and so does not materially affect quantitation at high *L. loa* microfilaremia (Hemilembolo and et al., 2023); however, unpublished data indicates that *M. perstans* loads can exceed 8000 mf/mL. The two filaria seem to have different patterns of movement in blood, which makes speciation in the videos potentially feasible. In addition, it is valuable to distinguish loiasis from LF because *L. loa* microfilariae can cause false positives in LF diagnostics that use microfilarial counts (however, this dataset contains no LF-positive cases).

5. Coagulation Once the blood capillary is loaded for imaging by the NTDscope device, the blood starts coagulating after a few minutes. This arrests filaria motion in the videos, leading to False Negatives for TaNT. Therefore a strong coagulation detection algorithm would improve safety in the TaNT use case.

4.2 Role of AI

Effective AI-driven automated diagnosis has potential to greatly improve the efficiency of diagnostics for all these use cases. First, it can mitigate the challenge of understaffing (insufficient numbers of trained microbiologists and laboratory personnel). Second, the NTDscope device enables rapid, on-the-spot diagnosis in the field, both eliminating the need to return blood samples to the lab for evaluation and also saving clinical teams much time. However, these benefits depend on effective detection algorithms tuned to the various use cases, and *L. loa* diagnostics (and NTD diagnostics generally) are currently underserved by the medical AI community. We hope this dataset enables development of AI solutions that can meet the stringent clinical requirements of the various filaria use cases, in order to accelerate progress in loiasis health care as well as other filarial diseases such as LF.

A baseline algorithm (hereafter "2026 algorithm") for *L. loa* detection on these videos is described in (Djune-Yemeli et al., 2026). It performs reasonably well for TaNT and quantitation, but has a high LoD, does not distinguish species, and does not detect coagulated blood samples. For baseline performance, see section 5.4. Interestingly, this algorithm uses no AI; rather, it leverages biophysical priors and applies image processing and statistical methods. Therefore an opportunity exists to apply current AI methods to develop improved *L. loa* detection algorithms.

4.3 Data location, licensing, validation

The dataset is available at Zenodo:

`https://zenodo.org/records/21517727`,

DOI 10.5281/zenodo.21517727, under the Creative Commons license: CC-BY 4.0: Attribution 4.0 Int'l `https://creativecommons.org/licenses/by/4.0/deed`. The videos are the raw .mp4 data, downsampled (2× decimation) using Python and openCV (Python Software Foundation; Bradski, 2000). For ground truth QC, see sections 4.5 and 5.6.

4.4 Ethical Considerations

Studies in Cameroon received ethical clearance from the Centre Regional Ethical Committee for Research on Human Health (CRERSH-Ce) and administrative authorization from the Centre Regional Delegation for Public Health of the Ministry of Public Health (CEIs 0094/CRERSHC/2023, 00934/CRERSHC/2025. Study population was first informed through the local health system (Health District, Health areas and community health personnel, community leaders...). In each community, all eligible individuals were invited to a central point (health facility or chieftaincy). An introductory speech was given by a team member and translated into a local language by community health personnel. All the potential participants were given the opportunity to ask questions before making the decision whether to participate or not. Consent/assent/parental consent forms were signed by all the participants.

The Gabon study was approved by the ethics committee of CERMEL under the number CEI-026/2022. Participants or their legal representatives gave informed consent before any study related procedures were performed.

The data has been deidentified according to the guidance of the clinical teams and HIPAA standards.

4.5 Dataset acquisition

All videos in this dataset were collected with the NTDscope device. Site details are as follows:

Cameroon Sample collection involved both the NTDscope test and Calibrated Thick Blood Smears (CBTS) in parallel. NTDscope testing on finger-prick blood, followed procedures in (D'Ambrosio et al., 2015). In parallel, CTBS were prepared using 70 µL of finger-prick blood, following standardized protocols of the ISM laboratory. Briefly, non-heparinized finger-prick blood was collected and drawn onto a microscope slide. The slide was then allowed to dry and stained with 10% Giemsa using standard procedures (Walther and Muller, 2003). For CBTS, on each stained slide 50 µL (not 70 µL) of blood was examined under a light microscope at 10X objective for blood dwelling mf. All mf present on the smear were counted and reported. Mf of *M. perstans*, also endemic in the study area, were distinguished from those of *L. loa* by size and the absence of a sheath. The final result was expressed in microfilariae per milliliter of blood (mf/mL) (WHO, 1991).

Gabon Recruitment for sampling was conducted at the Centre de Recherches Médicales de Lambaréné (CERMEL), in Moyen Ogooue (Ekouk, Nzong Mbang, Petit Odavo) and Ngounie (Sindara) provinces of Gabon, from 13 August 2023 to 24 August 2024. The region is highly endemic for *L. loa* and a range of other parasitic infectious diseases (Veletzky et al., 2020; Zoleko Manego et al., 2017; Ramharter et al., 2021). Participants for this study were from Lambarene and surrounding villages and Sindara.

5. Methods: Dataset contents

5.1 General organization

The data structure follows a nested hierarchy: Site, session, video. There are five *sites*: three Cameroon studies at different times, and two sites in Gabon (the Cameroon studies collected cases in various communities, but each is treated as a single "site" for folder structure purposes). There is also a set of deliberately coagulated samples. The *session* is the crucial clinical unit. It contains 7 videos of a capillary of blood from a single patient, and is the basis for patient diagnosis. The *videos* capture successive non-overlapping Fields of View (FoVs) along the capillary. In this dataset, patients have 1 to 4 sessions depending on the study protocols. Videos are 5 seconds long, captured at 15 to 35 frames per second (FPS). FoV size is about 4.5 mm $\times$ 6.2 mm and contains an estimated 3.75 μL of blood. The original image (i.e. frame) size is 1080 $\times$ 1440 $\times$ 3 (height $\times$ width $\times$ channels), with pixel pitch $\approx$ 4.3 μm / pixel. 2026 algorithm experiments indicated that frames can be downsampled by 3$\times$ (to 360 $\times$ 480 $\times$ 3) with no harm to algorithm performance but with great increase in processing speed. The videos in this dataset have been downsampled 2$\times$ by simple subsampling (to 540 $\times$ 720 $\times$ 3) to reduce file size (required for storage on Zenodo). To access the collection of deidentified full-sized videos ($\approx$280 GB) please contact the Fletcher Lab at University of California, Berkeley (fletch@berkeley.edu).

Each session has its own folder, named according to the following scheme: "site_patient_table" or "site_patient"

"site" can have the following values:
- "camJuly" (Cameroon July 2023)
- "camOct" (Cameroon October 2023)
- "camMay" (Cameroon May 2025)
- "sind[Sc, Pv]" (Sindara, Gabon, 2023). "Sc" and "Pv" refer to "screening" and "patient visits".
- "lamb[Ek, Nz, Po, Tr]" (Lambarene, Gabon, 2023). "Ek", "Nz", "Po" and "Tr" refer to local collection sites.
- "camJulyCoag", "camMayCoag" (coagulated sessions)

"patient" is a number with three digits (for "camJuly", "sind", and "lamb"); or with four digits (for "camOct" and "camMay") including leading zeros as needed.

"table" Table tags exist for two sites only: "camMay" and "camOct". The tags distinguish the multiple sessions from each patient. Details are in the "Per site details" section.

Each session folder contains seven .mp4 videos. Video filenames have the form: "site_patient_video#_focusDepth_timestamp", where "site_patient" matches the session folder name. Video filenames do not include "table" information.

"video#" is 1 to 7 where "1" is imaged first. Video FoVs step along the capillary.

"focusDepth" is an integer 0 to 300. It's the distance in microns of the camera's focus plane below the top surface of the capillary. This might hold relevance because the magnification changes slightly depending on focal depth. Also, "0" or "300" could indicate out-of-focus images.

"timestamp" has the form "hhmmss" (the date has been removed). The timezone is local.

5.2 Per-site details

Summary statistics for all sites are given in **Table 1**.

5.2.1 Cameroon July 2023 ("camJuly")

Videos are in the folder "july2023Cameroon". There are 50 sessions, one per patient, from 5 devices (a subset of those used in "camOct"). The device ID for each session is recorded in "july2023CameroonMetadata.xlsx". The distribution of *loa* filaremias is shown in Fig 3.

5.2.2 Cameroon October 2023 ("camOct")

Videos for 3397 sessions from 1147 patients are in the folder "october2023Cameroon". This study had a uniquely complex protocol (Fig 1) that yielded four sessions per patient: two from a single capillary run through the same device twice (to get intradevice variability on a single capillary), and two from a pair of capillaries, run through two devices.

The 4 sessions per patient are notated by "tables" (in the sense of a workstation where the blood draw was done) A1, A2, BC1, BC2. Due to an upload glitch in the deployed devices, some sessions are missing from this dataset, as follows: Number of sessions per table (out of a possible 1147): A1 has 770; A2 has 723: BC1 has 1101; BC2 has 803 Number of sessions per patient (out of a possible 4): 19 patients have 0; 112 have 1; 286 have 2; 307 have 3; 523 have all 4 sessions.

Three of the tables (A1, BC1, and BC2) can be considered "normal" and equivalent. BC1 and BC2 sessions are from two capillaries filled from the same finger prick, both run concurrently. Table A1 is from a different finger prick (in the other hand), run concurrently with BC1 and BC2. Thus, the variation in a single patient's *loa* burdens in these three sessions is normal. Table A2 sessions were the result of the A1 capillary being run a second time on the same device. Due to the time delay, A2 sessions have a markedly higher incidence of coagulation, which can begin after just a few minutes. The variation between a patient's A1 and A2 might be due to coagulation.

"camOct" metadata includes annotations of coagulation in videos and a dataset for training coagulation detection models. For more details see subsection 5.5. There were 13 devices used. The device ID for each session, along with demographic metadata are found in "october2023CameroonM
There are two expert microscopy reads, on Giemsa-stained blood films from different finger pricks. Intra-patient variation is expected [4], and is shown in Fig 2A. Cumulative distribution functions of the *loa* and *perstans* filaremias are given in Fig 3.

5.2.3 Cameroon May 2025 ("camMay")

Videos for 1011 sessions from 550 patients are in folder "may2025Cameroon". Most patients have two sessions, with different capillaries and devices. These are labeled as tables "A" and "B". There were 14 devices (the same as used in "camOct", but not mappable due to naming differences). The device IDs per session and demographic metadata are in "may2025CameroonMetadata.xlsx". *M. perstans* presence and counts are not captured. The distribution of the *loa* filaremias is shown in Fig 3.

5.2.4 Gabon 2023 ("lamb", "sind")

Videos for 217 sessions are in the folder "gabon2023". There were two main sites: Lambarene and Sindara. Lambarene had four sub-sites: Ekouk, Nzemba, Petit Odavo, and Tranquille. A few Ekouk patients returned for later visits (can be considered distinct cases). Thus the tags for Lambarene sessions are lambEk, lambNz, lambOd, lambTr, and lambPv (for "Patient Visit"). There is no "table" tag. Sindara has one session per patient and no "table" tag. The distributions of *loa* filaremias are shown in Fig 3.

5.2.5 Deliberately coagulated sessions

Ten patients from "camJuly" and "camMay" had a capillary run through the device repeatedly to study coagulation. These 34 sessions are found in the folder "coagulationExperiments". There is no metadata file. The timestamps on these videos offer valuable insight into coagulation times.

5.3 Recommended train/test splits

We recommend "camOct" as a training set, with table A1 either removed totally due to coagulation risk, or culled selectively via the methods in section 5.6.4.

We recommend "camMay" as a test set (except for speciation). It has many high filaremia cases suitable for TaNT. "camJuly" and Gabon are suitable test sets for mapping, speciation, and new-site generalization, but lack high

Site	Cameroon July 2023	Cameroon Oct 2023	Cameroon May 2025	Gabon 2023 Lambarene	Gabon 2023 Sindara
Site tag	camJuly	camOct	camMay	lamb	sind
# patients	44	1147	550	85	122
# sessions	46	3397	1011	95	122
# Giemsa reads per patient	1	2	1	1	1
# sessions per patient	1	1 - 4 *	2	1	1
% Female	60	49	49	-	-
Ages: mean ± std dev	43.2 ± 22.6	44.7 ± 20.6	47.2 ± 18.5	-	-
# *loa*-negative patients	31	788	353	70	85
# *loa*-positive patients	13	352	197	19	24
loa count range (mf/mL)	380-27,400	20-133,180	20-123,980	20-77,980	40 – 13,940
# patients with *loa* ≥ 30,000 mf/mL	0	31	33	1	0
# *perstans*-negative patients	40	984	-	88 **	98
# *perstans*-positive patients	4	156	-	1 **	11
perstans count range (mf/mL)	40 - 400	20 - 7580	-	100	10 - 560
# *loa* + *perstans* coinfections	0	79	-	0	5
# video with quality notes	25/308	many	0	all	all
# videos with manual mf counts	all	many	0	all	all

Table 1: Summary statistics for all sites. There are also 34 deliberately coagulated sessions. *For details see section 5.2.2. **10 patients have missing *perstans* reads (likely 0).

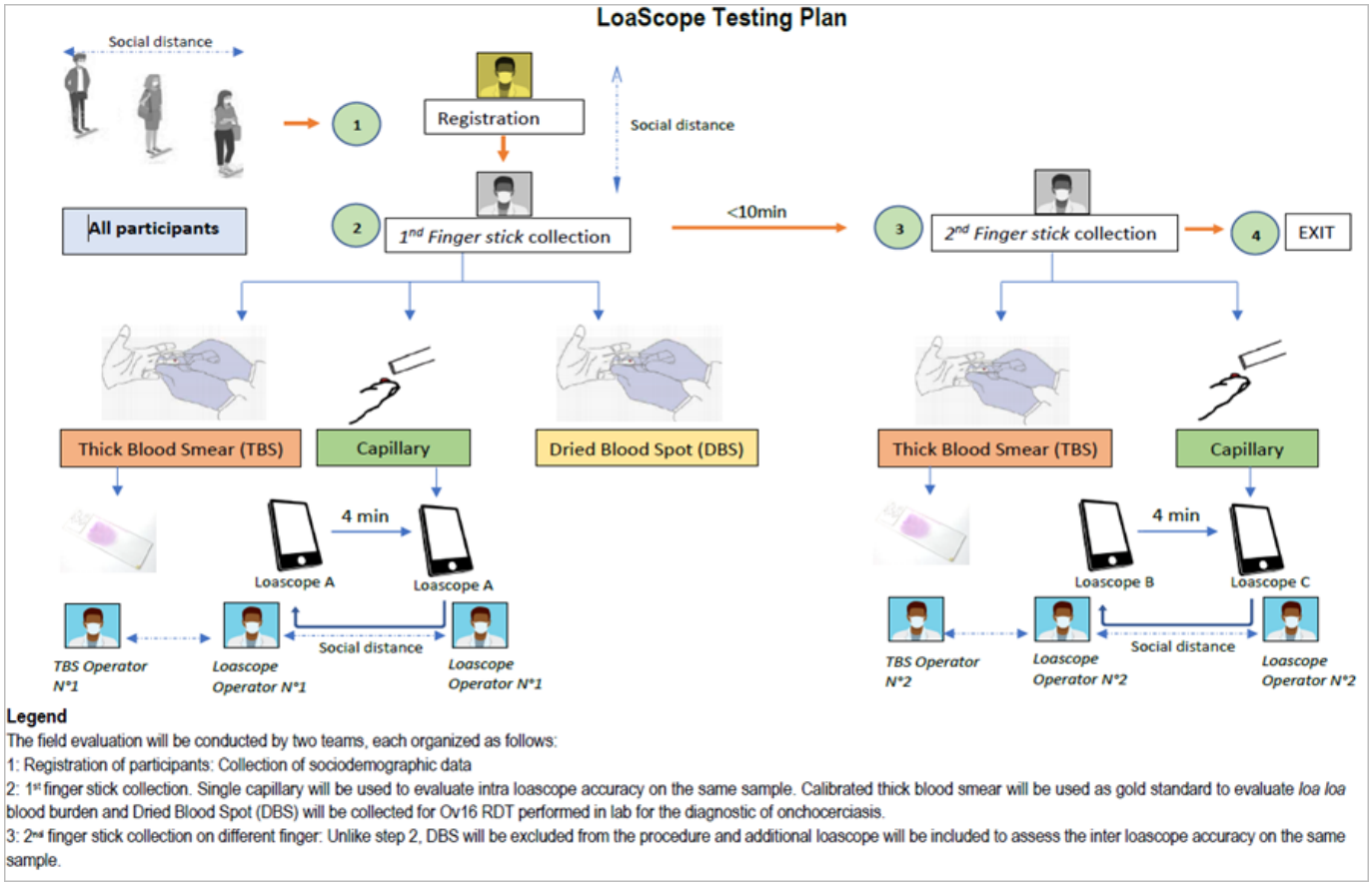

Figure 1: Protocol for "camOct". The righthand path gave two sessions, one from each of two capillaries (labeled as "tables" BC1 and BC2). The lefthand path gave two consecutive sessions from a single capillary ("tables" A1, A2).

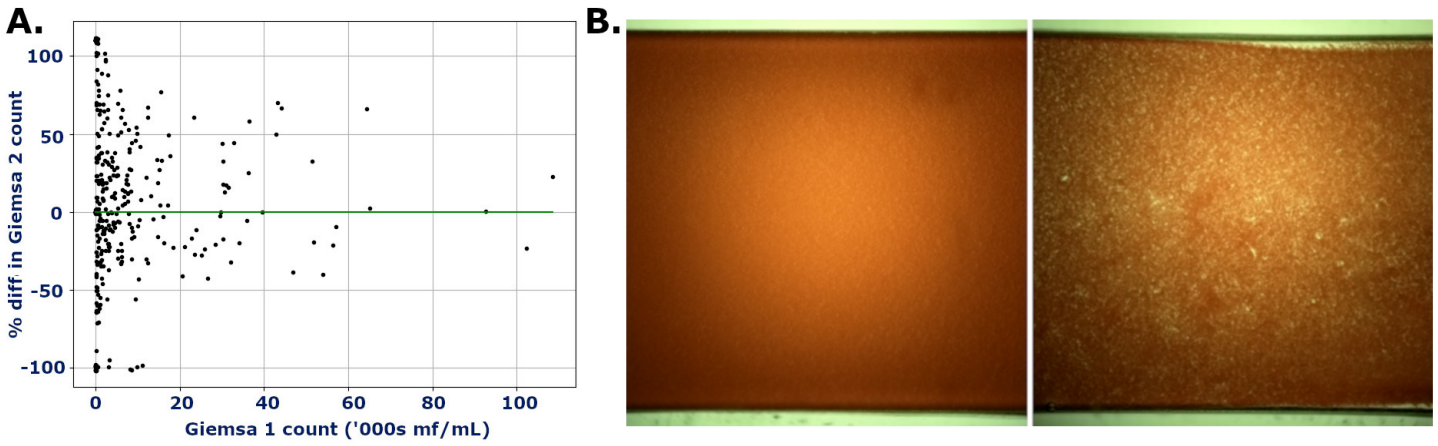

Figure 2: **A**: Intra-patient Giemsa read variability, *loa* only (*perstans* counts ignored), from "camOct": percent difference of Read 2 from Read 1 as reference, i.e. 100 $\frac{(read2-read1)}{read1}$. Values >100 were clipped to 100, then all y-axis values were slightly jittered. **B**: Normal (left) and Coagulated (right) video frames. Most videos in the dataset look normal, but table "A2" of "camOct" has videos spread between these two extremes.

filaremia cases for TaNT.

5.4 Baseline algorithm results

Performance metrics of the 2026 algorithm (trained and calibrated on "camOct") on "camMay" as a holdout set are shown in Table 2; further detail can be found in (Djune-Yemeli et al., 2026). The limit of detection was 750 - 1200 mf/mL due to false positives from bulk motion. Quantitation results are for patients with Giemsa > 1200 mf/mL. For comparison, inter-reader Giemsa discrepancies (absolute standard error) on "camOct" patients with > 1200 mf/mL had mean ± std dev = 26% ± 19% or 30% ± 24% (depending on which read is the reference); see also Fig 2A.

Task / Statistic	read A	read B
TaNT:		
Sensitivity[1]	94	97
Specificity[2]	97	97
Detect > 0 mf/mL (pos/neg):		
Sensitivity	92	91
Specifity	66	71
Detect > 1200 mf/mL:		
Sensitivity	98	99
Specificity	94	94
Quantitation error[3]:		
Mean	35	40
Std dev	34	37

Table 2: Baseline performance of the 2026 algorithm on "camMay" as holdout, for two NTDscope reads ("A" and "B"). All values are percentages. [1]Correctly flagged as "Not Treat" (errors on this risk SAEs). [2]Correctly flagged as "Treat". [3]Absolute standard error = $100\,|\frac{estimate-true}{true}|$; calculated on cases with >1200 mf/mL.

5.5 Failure modes

Some videos show certain failure modes, listed below. Quality and Coagulation annotations identify some of these videos (see section 5.6), especially in "camOct".

Bulk motion Ideally, the blood in the capillary is motionless, except as disturbed by swimming mf, and the only perturbation of pixel values from frame to frame is due to mf. However, in the Cameroon 2023 dataset, several videos contained regions of flowing blood ("bulk flow") due presumably to leaky capillaries. This flow creates perturbations from frame to frame, creating risk of erroneous mf detections. In a similar effect from different cause, bumping the device during imaging can induce bulk motion (e.g. a ripple-in-pond effect).

Flickering illumination In a few cases, videos appeared to have a flickering effect. This would cause pixel value differences and thus apparent motion which might risk erroneous mf detections.

Coagulation If the capillary is not imaged soon enough, the blood can begin to coagulate, which prevents movement by the mf (heparinized blood is not logistically practical). This leads to False Negative samples in the TaNT use case. A common visual difference between coagulated and liquid samples is, roughly speaking, that liquid samples have a more uniform orange color, while coagulated samples have a more "checkerboard" pattern of white and red, since as the blood coagulates it pulls away from small regions in the capillary (see Fig 2B). This was mainly seen in table A2 of the "camOct" study, due to the unique pro-

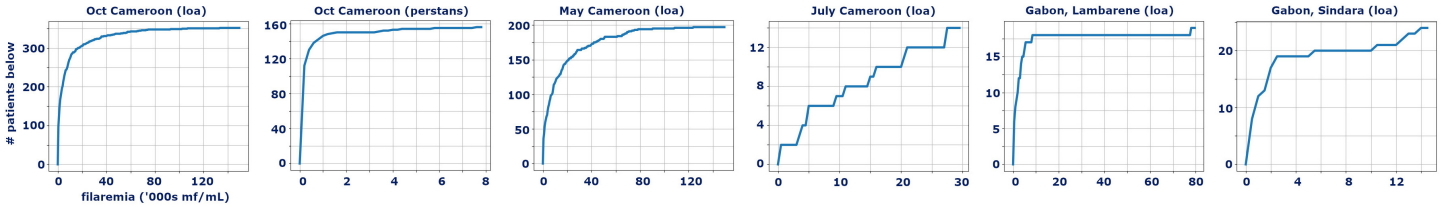

Figure 3: Filaremia cumulative distribution functions. x-axis = filaremia, y-axis = # patients below that value. L to R: "camOct" (*loa*), "camOct" (*perstans*), "camMay" (*loa*), "camJuly" (*loa*), Lambarene (*loa*), Sindara (*loa*).

tocol.

5.6 Ground truth data

There are four types of ground truth for sessions and videos:

1. Patient-level Giemsa counts (all sessions)
2. Manual counts of mf per video (some videos)
3. Manual quality annotations per video
4. Manual coagulation labels per video (some videos)

5.6.1 Giemsa counts per patient

The most important ground truth, corresponding to current clinical practice, is mf count (mf/mL) on Giemsa-stained blood films. All patients have an expert mf count by microscopy on 50 μL of Giemsa-stained blood from the same finger prick as the capillary fill, but not the actual blood that entered the capillaries.

An important aspect of this ground truth is variability: Intersample variability in mf counts from synchronous samples (e.g., from one finger prick, from two finger pricks from same or different hands, etc) is not well characterized but is known to be potentially high (Gardon et al., 1997). The "camOct" study, uniquely, had two Giemsa counts from synchronous finger pricks from different hands, giving insight into Giemsa count variability (Fig 2A). The Giemsa counts are found in (spreadsheet / sheet):

- july2023CamMetadata.xlsx / fieldMetadata
- oct2023CamMetadata.xlxs / fieldMetadata, also / algorithm_mfPerML_perTable
- gabon2023Metadata.xlsx / *_Giemsa
- may2025CamMetadata.xlsx / fieldMetadata

5.6.2 Manual counts per video

For some of the videos, humans watched the videos and counted the visible mf motion paths (they did not mark the x-y locations). These counts are not perfect, especially when the video contains over 30 mf since accurate tracking becomes difficult. The manual counts are significantly lower per volume of blood than the Giemsa counts, because the capillaries appear to have a sieving effect so that the count of mf inside a capillary is about 50% of the count in the original blood sample. The per-video counts are found in:

- july2023CamMetadata.xlsx / humanMfPerVid_Quality_Device
- oct2023CamMetadata.xlsx / humanMfPerVideo_qualityNotes
- gabon2023Metadata.xlsx / *_humanMfPerFov

5.6.3 Quality annotations per video

Many videos in the "camOct" and Gabon studies were manually inspected for quality issues, such as the failure modes described above. These notes are found in:

- july2023CamMetadata.xlsx / humanMfPerVid_Quality_Device
- oct2023CamMetadata.xlsx / humanMfPerVideo_qualityNotes
- gabon2023Metadata.xlsx / *_Quality

5.6.4 Coagulation labels per video

If there is a time delay (roughly >3 - 4 minutes) between blood draw and imaging, blood can coagulate in the capillary before or during imaging. Identifying coagulation is important to: (i) flag unreliable field results; (ii) properly interpret undercounting errors in filaria detector algorithms (mf are undetectable in coagulated videos due to lack of motion); and (iii) assemble train-test sets for coagulation detector dev. There are five sources for coagulated videos:

1. 62 complete sessions from "camOct" were manually annotated for coagulation with labels "normal", "coagulated", or "interim", listed in coagulationOct2023Cam.xlsx. The videos in a given session can have different labels (if the blood was coagulating during imaging). "Interim" labels might be omitted from the train set for a video classifier because their status is unclear. For realistic validation, all 7 of a session's videos should be checked, and the session should receive a "coagulated" label if even one of its videos is labeled as coagulated. The train-test split is stratified by session. This set can be readily expanded by applying criteria 2 - 5 below.

2. Use the deliberately coagulated sessions (see 5.2.5).

3. Compare algorithm vs Giemsa mf counts (positive patients only): If a session's algorithm count is much lower than its Giemsa count, it is a suspect for coagulation. Con-

versely, for positive patients, if a session's algorithm count is higher or similar to the Giemsa count, then it is likely uncoagulated (unless the session exhibits bulk motion or illumination flicker, as described in "Session failure modes" above, since these can produce erroneous high counts by the 2026 algorithm).

4. Table A2 of "camOct" are good candidates for coagulation, due to the time delays in the protocol.

5. A few Gabon videos exhibit coagulation, as listed in gabon2023Metadata.xlsx / *_Quality

Acknowledgments

Our heartfelt thanks to all the generous participants in these studies.
CBD, ALN, ES, DB, MDK were supported by Global Health Labs, LLC. Cameroon data collection was funded by Global Health Labs, LLC.

Conflicts of Interest

IIB consults to the Weapons Threat Reduction Program at Global Affairs Canada. The other authors declare that we have no conflicts of interest.

References

C. Boulle, S.D. Pion, M. Boussinesq, and alia. Revisiting the *Loa loa* microfilaremia thresholds above which serious adverse events may occur with ivermectin treatment. *PLoS Neglected Tropical Diseases*, 2025.

M. Boussinesq. Loiasis. *Annals of Tropical Medicine & Parasitology*, 100:715–731, 2006. .

M. Boussinesq, J. Gardon, N. Gardon-Wendel, and J-P. Chippaux. Clinical picture, epidemiology and outcome of Loa-associated serious adverse events related to mass ivermectin treatment of onchocerciasis in Cameroon. *Filaria Journal*, 2003.

G. Bradski. The OpenCV Library. *Dr. Dobb's Journal of Software Tools*, 2000.

K. G. Buell, C. Whittaker, M. Boussinesq, and alia. Atypical clinical manifestations of loiasis and their relevance for endemic populations. *Open Forum Infectious Diseases*, 6:ofz417, 2016. .

C. B. Chesnais, I. Takougang, M. Boussinesq, and alia. Excess mortality associated with loiasis: A retrospective population-based cohort study. *Lancet Infectious Diseases*, 17:108–116, 2017. .

M. V. D'Ambrosio, M. Bakalar, D.A. Fletcher, and alia. Point-of-care quantification of blood-borne filarial parasites with a mobile phone microscope. *Science Translational Medicine*, 2015.

M. de Leon Derby, Z.L. Moussa, D.A. Fletcher, and alia. NTDscope: A multi-contrast portable microscope for disease diagnosis, 2025.

L. Djune-Yemeli, C.B. Delahunt, J. Kamgno, and alia. Automated detection of *Loa loa*: a field trial in Cameroon. *In Review*, 2026. Preprint available on bioRxiv.org.

J. Gardon, N. Gardon-Wendel, M. Boussinesq, and alia. Serious reactions after mass treatment of onchocerciasis with ivermectin in an area endemic for *Loa loa* infection. *Lancet*, 1997.

J. Goldin and A. L. Juergens. Filariasis. In *StatPearls*. StatPearls Publishing, Treasure Island, FL, 2025.

M. C. Hemilembolo and et al. *Loa loa* and *Mansonella perstans* microfilaremia in the department of Lékoumou, Republic of Congo. *Parasites & Vectors*, 2023.

K.H. Jacobsen, B.C. Andress, A.S. Williams, and alia. A call for loiasis to be added to the WHO list of neglected tropical diseases. *Lancet Infectious Diseases*, 22(10): e299–e302, 2022. .

T. J. Kamtchum and alia. Epidemiology of *Loa loa* and *Mansonella perstans* filariasis in the Akonolinga Health District, Centre Region, Cameroon. *Health Sciences and Diseases*, 2014.

L. A. Kelly-Hope, M. Bockarie, and D. H. Molyneux. *Loa Loa* ecology in Central Africa: Role of the Congo River System. *PLoS Neglected Tropical Diseases*, 6:e1605, 2012. .

W. G. Metzger and B. Mordmüller. *Loa Loa*—does it deserve to be neglected? *Lancet Infectious Diseases*, 14: 353–357, 2014. .

S. D. S. Pion. Implications for annual retesting after a test-and-not-treat strategy for onchocerciasis elimination in areas co-endemic with *Loa loa* infection: an observational cohort study. *Lancet Infectious Diseases*, 2020.

Python Software Foundation. URL `https://www.python.org/`).

M. Ramharter, S. T. Agnandji, A. A. Adegnika, P. G. Mremsner, and alia. Development of sustainable research excellence with a global perspective on infectious diseases: Centre de recherches médicales de lambaréné (cermel), gabon. *Wiener klinische Wochenschrift*, 2021.

M. Ramharter, J. Butler, R. Zoleko Manego, and alia. The african eye worm: current understanding of the epidemiology, clinical disease, and treatment of loiasis. *Lancet Infectious Diseases*, 2024. .

L. Veletzky, J. Hergeth, D. R. Stelzl, M. Ramharter, and et alia. Burden of disease in Gabon caused by loiasis: a cross-sectional survey. *Lancet Infectious Diseases*, 2020.

L. Veletzky, K. A. Eberhardt, M. Ramharter, and alia. Analysis of diagnostic test outcomes in a large loiasis cohort from an endemic region: Serological tests are often false negative in hyper-microfilaremic infections. *PLoS Neglected Tropical Diseases*, 18(3):e0012054, 2024. .

M. Walther and R. Muller. Diagnosis of human filariases (except onchocerciasis). In *Advances in Parasitology*. Academic Press, 2003.

WHO. *Basic Laboratory Methods in Medical Parasitology*. World Health Organization, 1991. ISBN 92-4-154410-4.

WHO. Rapid assessment procedures for loiasis: Report of a multi-centre study. `http://54.213.233.103/static/uploaded_files/loiasis.pdf`, 2001.

WHO. Loiasis: A Very Neglected Disease in Central Africa. `https://www.who.int/news-room/events/detail/2025/12/04/default-calendar/loiasis--a-very-neglected-disease-in-central-africa`, 2025a.

WHO. Lymphatic filariasis. `https://www.who.int/health-topics/lymphatic-filariasis`, 2025b.

R. Zoleko Manego, G. Mombo-Ngoma, M. Witte, P. B. Matsiegui, and alia. Demography, maternal health and the epidemiology of malaria and other major infectious diseases in the rural department Tsamba-Magotsi, Ngounié Province, in central African Gabon. *BMC Public Health*, 2017.